Inorganic Chemistry

Article

pubs.acs.org/IC

DNA Cleavage by the Photocontrolled Cooperation of Zn^{II} Centers in an Azobenzene-Linked Dizinc Complex

Anangamohan Panja, Takashi Matsuo, Satoshi Nagao, and Shun Hirota*

Graduate School of Materials Science, Nara Institute of Science and Technology, 8916-5 Takayama, Ikoma, Nara 630-0192, Japan

Supporting Information

ABSTRACT: We synthesized a new photoactive dinuclear zinc(II) complex by linking two zinc centers with a ligand containing an azobenzene chromophore and investigated the DNA cleavage activities of its trans and cis forms. The trans structure of the dinuclear zinc complex was determined by X-ray crystallography, where each zinc center is situated in an octahedral coordination environment comprised of three nitrogen atoms from the ligand and three oxygen atoms from two nitrate ions. The dinuclear zinc complex containing the azobenzene chromophore was photoisomerizable between the trans and cis forms. The binding affinities of the trans and cis complexes with calf thymus (CT)-DNA were similar. Although the DNA cleavage activity of the trans complex was negligible, the cis complex was able to cleave DNA. We attribute the efficient activity of the cis complex to the cooperation of the two closely located zinc centers and the inactivity of the trans complex to the two metal centers positioned far away from each other. The DNA cleavage activity of the cis complex exhibited a pH-dependent bell-shaped profile, which has been observed in the hydrolytic cleavage of DNA by zinc complexes. The DNA cleavage activity was not inhibited by a major groove binder, methyl green, but decreased significantly by a minor groove binder, 4′,6-diamidino-2-phenylindole, indicating that the dinuclear zinc complex binds to the minor groove of DNA. The present work shows the importance of the cooperation of two zinc ions for hydrolytic DNA cleavage, which can be photoregulated by linking the two metal centers with a photoisomerizable spacer, such as an azobenzene chromophore.

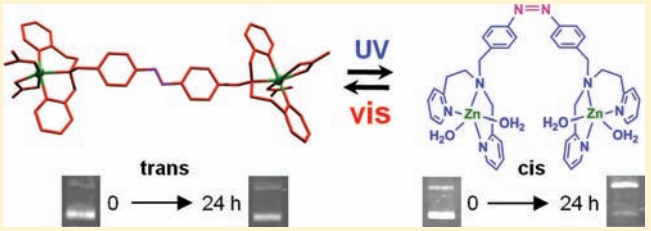

INTRODUCTION

Over the past few decades, the development of artificial DNA cleaving reagents has attracted considerable attention because of their practical applications in the fields of molecular biology, biotechnology, and chemotherapy.[1−7] The DNA cleavage reactions proceed by targeting various constituents of DNA, such as nucleic bases, the deoxyribose sugar moiety, and phosphodiester linkage. The oxidative DNA cleavage reaction generally involves nucleobase oxidation and/or degradation of the sugar moiety by the toxic radical species, which is generated by abstraction of the sugar hydrogen atom(s).[8−10] Oxidative cleavage also requires an additional reducing reagent, such as hydrogen peroxide or ascorbic acid. These properties limit the use of oxidative cleavage reagents to in vitro applications,[11−17] in which the modified DNA fragments produced by oxidative cleavage are not suitable for further enzymatic manipulation. In hydrolytic cleavage, the phosphodiester backbone is hydrolyzed.[18−21] The nucleic bases and deoxyribose sugar moiety are not modified, and no additional reagent is necessary when they are hydrolytically cleaved, which allows the cleaved fragments to be regulated enzymatically.[22−24] Therefore, small metal complexes that undergo hydrolytic DNA cleavage are useful in genetic engineering and molecular biotechnology.[25−27]

Many mono-, di-, and multinuclear metal complexes have been reported for DNA hydrolytic cleavage reactions.[28−36] Di- and multinuclear complexes are typically more reactive than their corresponding monometallic complexes for hydrolysis of a phosphodiester linkage because the metal centers in the di- and multinuclear complexes exhibit cooperation.[37,38] In fact, the extraordinary catalytic efficiencies of many natural nucleases rely on the cooperative actions of two or more metal ions.[39−45] Among various physiologically relevant metal ions, Zn^{II} is suitable for artificial metallonucleases because of the virtues of its strong Lewis acidity, high charge density, and rapid ligand-exchange ability. Zn^{II} exhibits a d^{10} electronic configuration, and the redox inertness rules out the possibility of oxidative cleavage. In addition, it generally has no ligand-field stabilization energy and, as a consequence, it can easily attain variable coordination numbers for water coordination during hydrolytic cleavage.

The intermetallic distance and rigidity of a dinuclear complex are important for the cooperation of the metal centers in DNA cleavage. Because azobenzene has been used to regulate the structure and distance in various systems,[46−57] we have previously linked two Cu^{II}-bound dipeptides with an azobenzene group, which could be photoisomerized between the trans and cis forms.[51] Two Cu^{II} centers were positioned relatively far away from each other in the trans complex, where no appreciable DNA cleavage activity was detected. In the cis complex, the Cu^{II} centers

Received: June 10, 2011
Published: October 26, 2011

were closely located, and the complex exhibited excellent DNA cleavage activity.

In this study, we linked two Zn^{II} centers with an azobenzene derivative to produce a photoactive hydrolytic DNA cleavage reagent **1**·Zn-*trans*/**1**·Zn-*cis* (Scheme 1). A neutral ligand was

Scheme 1. Photoisomerization of Complex 1·Zn[a]

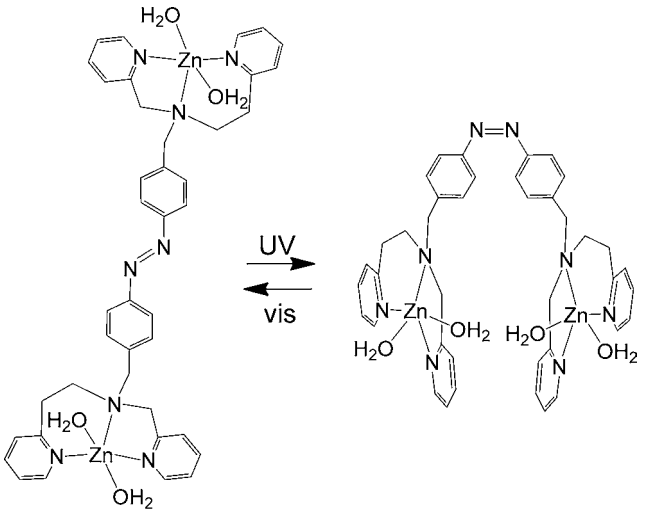

[a]Two Zn^{II} centers are interlinked with an azobenzene chromophore. The **1**·Zn-*trans* and **1**·Zn-*cis* isomers are converted to **1**·Zn-*cis* and **1**·Zn-*trans* by irradiation with UV and visible light, respectively.

synthesized to enhance the binding ability of the complex with DNA by increasing the electrostatic interaction. The cis form of the complex showed efficient DNA cleavage activity, while no significant DNA cleavage activity was observed for the trans complex. The higher activity of the cis complex is due to the cooperation of two closely associated Zn^{II} centers (Scheme 1). To the best of our knowledge, this is the first example for photoregulation of the cooperation between two Zn^{II} centers in DNA cleavage.

EXPERIMENTAL SECTION

Materials and Spectroscopic Measurements. Zinc nitrate hexahydrate, 4-nitrobenzyl alcohol, 2-pyridinecarboxaldehyde, 2-(aminoethyl)pyridine, and tris(hydroxymethyl)aminomethane (Tris) were purchased from Wako Pure Chemicals Industries, Ltd., Japan. Calf thymus (CT)-DNA, ethidium bromide (EB), methyl green, and 4′,6-diamidino-2-phenylindole (DAPI) were purchased from Sigma. Other chemicals and solvents were of analytical grade and were used without further purification.

Measurements of ^1H and ^{13}C NMR spectra were conducted using a JNM-ECP400 spectrometer (JEOL) in $CDCl_3$ or CD_3CN. If necessary, HMQC and HMBC measurements were carried out for the peak assignments. Electrospray ionization mass spectrometry (ESI-MS) was performed using a JMS-T100LC mass spectrometer (JEOL). Absorption spectra were measured using a UV-2450 spectrophotometer (Shimadzu) with a 1-cm-path-length quartz cell. Fluorescence experiments were performed with an F-4500 spectrofluorometer (Hitachi, Japan).

Synthesis of Ligand 1. 4,4′-Bis(chloromethyl)azobenzene and (2-pyridylmethyl)(2-pyridylethyl)amine were synthesized according to the reported methods.[52,58] 4,4′-Bis(chloromethyl)azobenzene (1.11 g, 4.0 mmol) and (2-pyridylmethyl)(2-pyridylethyl)amine (1.71 g, 8.0 mmol) were dissolved in 100 mL of *N*,*N*-dimethylformamide (DMF). After the addition of triethylamine (0.80 g, 8.0 mmol) and NaI (1.19 g, 8.0 mmol), the mixture was stirred at room temperature for 2 days. The solution was poured into ice−water, yielding a crude product. Recrystallization from a hexane−dichloromethane mixture afforded ligand **1** as a brownish-orange powder. Yield: 1.14 g (45%). ^1H NMR (400 MHz, $CDCl_3$): δ 2.96 (4H, t, J = 7.6 Hz, $-NCH_2CH_2C_6H_4N$), 3.04 (4H, t, J = 7.6 Hz, $-NCH_2CH_2C_6H_4N$), 3.76 (4H, s, $-NCH_2Py$), 3.84 (4H, s, $-NCH_2C_6H_4N{=}N-$), 7.07−7.14 (4H, dd, J = 11.5 and 6.3 Hz, Py5,5′), 7.26−7.36 (4H, m, Py3,3′), 7.42 (4H, d, J = 8.4 Hz, phenyl protons near the azo group), 7.55−7.59 (4H, m, Py4,4′), 7.81 (4H, d, J = 8.4 Hz, phenyl protons far from the azo group), 8.49 (4H, dd, J = 11.5 and 6.3 Hz, Py6,6′). ^{13}C NMR (100 MHz, $CDCl_3$): δ 36.77 ($-NCH_2CH_2Py$), 54.85 ($-NCH_2CH_2Py$), 58.92 ($-NCH_2Py$), 60.81 ($-NCH_2C_6H_4N{=}N-$), 121.80 (Py5 or 5′), 122.58 (Py5 or 5′), 123.29 (Py3 or 3′), 123.35 (Py3 or 3′), 123.38 (phenyl carbons near the azo group), 123.43 (phenyl carbons near the azo group), 129.97 (phenyl carbons far from the azo group), 130.38 (phenyl carbons far from the azo group), 136.81 (Py4 or 4′), 137.06 (Py4 or 4′), 143.42 (*ipso*-carbon bonding with the azo group), 149.50 (Py6 or 6′), 149.85 (Py6 or 6′), 152.52 (*ipso*-carbon far from the azo group), 160.65 (Py 2 or 2′), 161.15 (Py2 or 2′). ^1H NMR (400 MHz, CD_3CN): δ 2.87 (4H, t, J = 7.2 Hz, $-NCH_2CH_2C_6H_4N$), 3.00 (4H, t, J = 7.2 Hz, $-NCH_2CH_2C_6H_4N$), 3.76 (4H, s, $-NCH_2Py$), 3.79 (4H, s, $-NCH_2C_6H_4N{=}N-$), 7.07−7.14 (4H, m, Py5,5′), 7.33−7.39 (4H, m, Py3,3′), 7.46 (4H, d, J = 11.7 Hz, phenyl protons near the azo group), 7.61−7.68 (4H, m, Py4,4′), 7.79 (4H, d, J = 11.7 Hz, phenyl protons far from the azo group), 8.41 (2H, d, J = 6.4 Hz, Py6 or 6′), 8.46 (2H, d, J = 6.4 Hz, Py6 or 6′). ESI-MS (m/z, positive mode). Calcd for $C_{40}H_{41}N_8$ ($[M + H]^+$): 633.35. Found: 633.35.

Synthesis of the Zinc(II) Complex 1·Zn. Ligand **1** (0.632 g, 1.0 mmol) in 20 mL of methanol was added to $Zn(NO_3)_2{\cdot}6H_2O$ (0.595 g, 2.0 mmol) in 30 mL of acetonitrile. The resulting orange-yellow solution was refluxed for 1 h and filtered to remove the insoluble materials. By incubation of the solution at ambient temperature, a dark-yellow powder was generated. Yellow microcrystalline material was obtained by the slow evaporation of an acetonitrile−methanol solution after 1 week. ^1H NMR (400 MHz, CD_3CN): δ 3.23−3.33 (8H, m, $-NCH_2CH_2Py$), 3.91 (2H, d, J = 15 Hz, $-NCH_\alpha Py$), 3.98 (2H, d, J = 15 Hz, $-NCH_\beta Py$), 4.14 (2H, d, J = 14 Hz, $-NCH_\alpha C_6H_4N{=}N-$), 4.31 (2H, d, J = 14 Hz, $-NCH_\beta C_6H_4N{=}N-$), 7.42 (4H, d, J = 8.3 Hz, phenyl protons near the azo group), 7.51 (2H, d, Py3 or 3′), 7.59 (4H, m, Py5 or 5′), 7.65 (2H, m, Py3 or 3′), 7.94 (4H, d, J = 8.3 Hz, phenyl protons near the azo group), 8.02 (2H, m, Py4 or 4′), 8.13 (2H, m, Py4 or 4′), 8.75 (4H, m, Py6 and 6′). ESI-HR-MS (m/z, positive mode). Calcd for $C_{40}H_{40}N_{11}O_9Zn_2$ ($[\mathbf{1}{\cdot}Zn - NO_3]^+$): 946.15934. Found: 946.15948.

X-ray Analysis. Single crystals suitable for X-ray diffraction were obtained by the slow diffusion of ether into an acetonitrile solution of the dinuclear complex **1**·Zn. X-ray diffraction intensity data were collected with a Rigaku RAXIS RAPID (3 kW) imaging plate area detector with graphite-monochromated Mo Kα radiation (λ = 0.710 73 Å) in the ω–2θ scanning mode. A single crystal was mounted at the top of a glass fiber and collected at 123 K in a stream of gaseous nitrogen. The reflection data were corrected for Lorentz and polarization effects. The structure was solved by direct methods and refined on F^2 by full-matrix least-squares techniques with the *SHELXL-97* program.[59] All of the non-hydrogen atoms were refined anisotropically, and all of the hydrogen atoms belonging to the complex were fixed in their calculated positions and refined using a riding model. Calculations were performed with the Rigaku *Crystal Structure 4.0* software package. A summary of the crystallographic data for complex **1**·Zn is listed in Table 1.

Photoisomerization Experiments. The UV light (320 nm < λ < 400 nm) was obtained by a 150-W xenon lamp (Hamamatsu Photonics) using a combination of UV pass (280 nm < λ < 400 nm) and sharp-cut filters (λ < 320 nm). The visible light (λ > 420 nm) was obtained by the same light source using a sharp-cut filter (λ < 420 nm). Irradiation of ligand **1** in $CDCl_3$ and complex **1**·Zn in D_2O with UV and visible light was performed for the trans-to-cis and cis-to-trans photoisomerizations, respectively. Determination of the trans/cis ratio of ligand **1** was done by calculating the relative intensities of the shifted

dx.doi.org/10.1021/ic201244y | *Inorg. Chem.* 2011, 50, 11437–11445

Table 1. Crystallographic Data and Structure Refinement for Complex 1·Zn in the Trans Form

empirical formula	$C_{40}\ H_{40}\ N_{12}\ O_{12}\ Zn_2$
fw	1011.59
temperature (K)	123(2)
wavelength (Å)	0.710 73
cryst syst	monoclinic
space group	$P2_1/n$
unit-cell dimens	
a (Å)	8.387(6)
b (Å)	14.336(8)
c (Å)	18.687(10)
β (deg)	96.537(3)
volume (Å^3)	2234.6(4)
Z	2
D_{calc} (g cm^{-3})	1.503
μ (mm^{-1})	1.149
$F(000)$	1040
θ range (deg)	3.04−25.38
reflns collected	31 196
indep reflns	4075
refinement method	full-matrix least squares on F^2
data/restraints/param	4075/0/298
GOF on F^2	1.054
final R indices [$I > 2\sigma(I)$]	R1 = 0.102, wR2 = 0.229
largest diff peak and hole (e Å^{-3})	0.57 and −0.43

signals at about 6.75 (corresponding to the cis form, four protons) and 7.42 ppm (trans form, four protons) against the less-sensitive ones at about 8.49 ppm (cis and trans forms, four protons) by photoisomerization. The stability of the cis form (cis-to-trans thermal isomerization rate) of complex **1**·Zn in the absence and presence of DNA was elucidated by observation of the UV−vis spectral changes in an aqueous solution or a 20 mM phosphate buffer (pH 7.5) at 37 °C.

Binding of Zinc(II) Complex to CT-DNA. The binding properties of dinuclear complex **1**·Zn to DNA were examined by UV−vis and fluorescence spectroscopies. The ratio between the UV absorbances of CT-DNA in a 20 mM phosphate buffer (pH 7.5) at 260 and 280 nm was about 1.9, indicating that DNA was sufficiently free from protein. The concentration of CT-DNA in base pairs was calculated using its molar absorption coefficient value of 6600 M^{-1} cm^{-1} at 260 nm.[60] Complex **1**·Zn (2.5×10^{-5} M) was titrated with varying concentrations of CT-DNA (up to about 1.2×10^{-4} M), and the changes in the absorption spectra were recorded after incubation for 5 min.

The relative binding affinity of the complex to CT-DNA was studied using the fluorescence spectral technique with EB-bound CT-DNA (2.5×10^{-5} M) in a 20 mM phosphate buffer (pH 7.5). The changes in the fluorescence intensity at 600 nm (526 nm excitation) of EB-bound CT-DNA were recorded at each incremental addition of the complex [$(0-5.0) \times 10^{-5}$ M].

DNA Cleavage Experiments. Plasmid DNA (pUC19) was extracted by overexpression in *Escherischia coli* DH5α cells, and the obtained DNA was purified with a QIAGEN kit (QIAprep spin miniprep kit-250). A DNA stock solution was prepared in a 10 mM Tris buffer (pH 8.0). The purity of DNA was checked by gel electrophoresis. Then, DNA was stored at 4 °C until use. The DNA cleavage activity of complex **1**·Zn was determined by monitoring the conversion of supercoiled plasmid DNA (form I) to nicked-circular DNA (form II) using agarose gel electrophoresis. **1**·Zn-*cis*-pss was obtained by irradiation of 4.0 mM **1**·Zn-*trans* with UV light in an aqueous solution for 1 h and used immediately after irradiation. The experiments were carried out by incubation of the reaction mixtures containing about 1 μg of DNA and compound **1**·Zn, in a 20 mM phosphate buffer (~350 ± 50 μL) at 37 °C. A mixture of equal volumes of a 10 × DNA loading buffer (Takara-bromophenol blue) and a 10 mM ethylenediaminetetraacetic acid (EDTA) aqueous solution was used to quench the DNA cleavage reaction, where 4 μL of the mixed solution was added to 18 μL of the reaction solution. The quenched samples were loaded to 1% agarose gel, and electrophoresis was carried out for 40−60 min at 100 V using a Tris-acetate-EDTA buffer (pH 8.0). After electrophoresis, the gel was transferred to an EB solution (1 μg/1 μL) and stained. The bands of the supercoiled and nicked-circular DNA forms were visualized using a gel document instrument (ChemiDoc XRS, Biorad). The intensities of the supercoiled plasmid DNA bands were multiplied by a factor of 1.3, to compensate for its weaker staining capability with EB compared to the nicked-circular form.[61,62] To determine the DNA interaction center of complex **1**·Zn, the supercoiled plasmid DNA was pretreated with a major groove binder, methyl green (50 μM),[63] or a minor groove binder, DAPI (50 μM),[64] at room temperature for 30 min before the addition of complex **1**·Zn.

RESULTS AND DISCUSSION

Synthesis and Characterization. The synthetic route for the preparation of ligand **1** is depicted in Scheme 2. The

Scheme 2. Syntheses of Ligand 1 and Its Dinuclear Zinc Complex 1·Zn

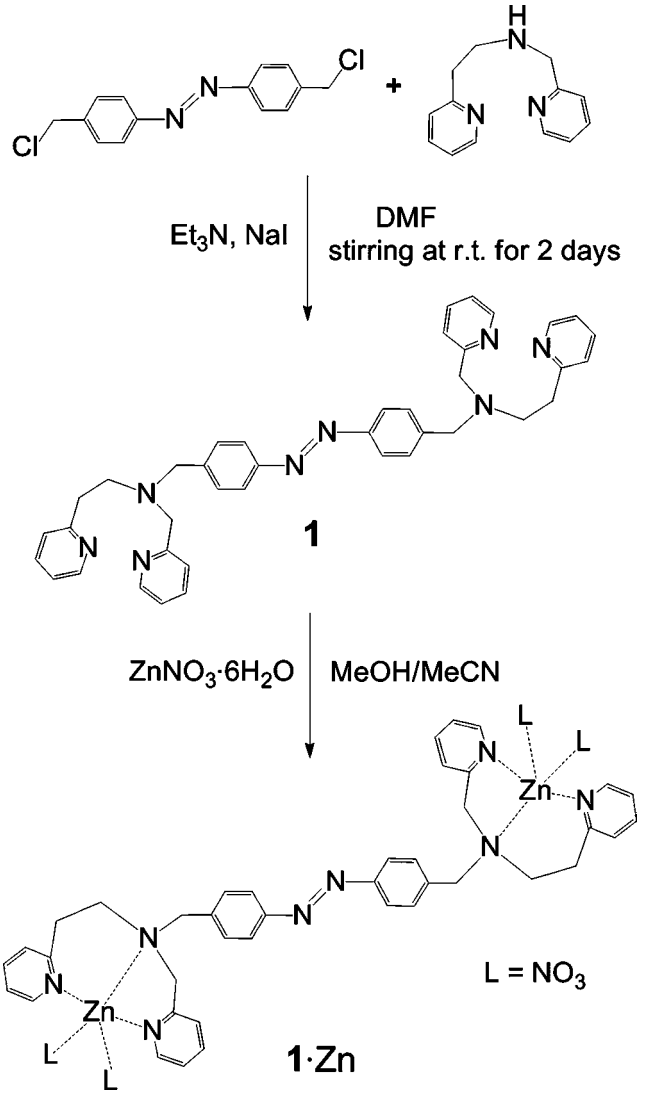

nucleophilic substitution of the chloride atoms of 4,4′-bis-(chloromethyl)azobenzene with (2-pyridylmethyl)(2-pyridylethyl)-amine in the presence of sodium iodide and triethylamine resulted

dx.doi.org/10.1021/ic201244y | Inorg. Chem. 2011, 50, 11437−11445

in the production of ligand **1** in good yield. The ligand was characterized by ESI-MS, ^{1}H NMR, and UV−vis methods. The treatment of ligand **1** with zinc nitrate produced complex **1**·Zn. Zinc complexation was confirmed by the ESI-MS and ^{1}H NMR measurements (see the Experimental Section and Figure S1 in the Supporting Information): The peaks for the aromatic protons in the NMR spectrum showed a downfield shift, indicating that the π-electron density was distributed to the added Zn^{2+} cations. Several pyridine protons became magnetically anisotropic. Furthermore, geminal coupling was observed for the pyridylmethyleneamine and azobenzenemethylene moieties. These properties suggest that the conformational restriction of the ligand increased by incorporation of the Zn^{2+} cation. The obtained complex was highly soluble in dimethyl sulfoxide and DMF and partly soluble in water, methanol, and acetonitrile. The complex exhibited a characteristic absorption band at 337 nm, indicating a trans configuration around the N═N bond (vide infra).

Crystal Structure of 1·Zn in the Trans Form. The structure of complex **1**·Zn in the trans form (**1**·Zn-*trans*) was determined by the single-crystal X-ray diffraction technique. Crystallographic data and details of data collection and refinement for **1**·Zn-*trans* are listed in Table 1. The important bond lengths and angles are summarized in Table 2. Complex

Table 2. Selected Bond Lengths (Å) and Angles (deg) of Complex 1·Zn in the Trans Form

Zn1−N1	2.228(7)	Zn1−N2	2.068(8)
Zn1−N3	2.058(8)	Zn1−O1	2.091(8)
Zn1−O2	2.468(7)	Zn1−O4	2.128(8)
O1−Zn1−O4	113.1(3)	O1−Zn1−N1	150.8(3)
O1−Zn1−N2	90.7(3)	O1−Zn1−N3	93.1(3)
O4−Zn1−N1	94.6(3)	O4−Zn1−N2	94.1(3)
O4−Zn1−N3	100.7(3)	N1−Zn1−N2	77.6(3)
N1−Zn1−N3	90.7(3)	N2−Zn1−N3	161.8(3)
O1−Zn1−O2	55.1(3)	O1−Zn1−O4	113.1(2)
O2−Zn1−N1	96.4(3)	O4−Zn1−N1	94.5(2)
O2−Zn1−O4	167.4(3)		
Zn1···Zn1a	17.872 (1)	C14···C14a	12.08(1)

1·Zn crystallized in the monoclinic $P2_1/n$ space group, where the asymmetric unit corresponded to half of the molecule. Each Zn^{II} ion of the two centrosymmetrical metal centers was coordinated with two pyridine nitrogen atoms and one tertiary amine nitrogen atom from one arm of ligand **1** and three oxygen atoms from two nitrate ions (Figure 1).

A nitrate ion can bind to the metal center in monodentate and bidentate fashions. We were able to use the difference in

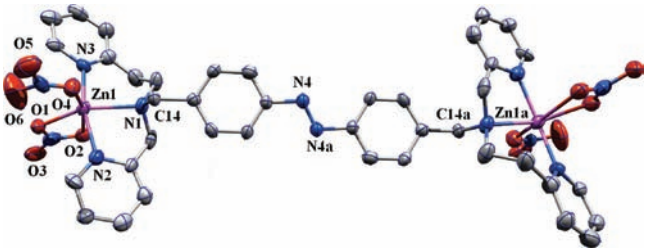

Figure 1. Molecular structure of complex **1**·Zn in the trans form. The structure is shown in an atom-labeling scheme. Hydrogen atoms are omitted for clarity (ORTEP, 30% ellipsoids).

the M−O distance (Δd) to classify the nitrate denticity: Δd < 0.3 Å for bidentate; 0.3 Å < Δd < 0.6 Å for anisobidentate; Δd > 0.6 Å for monodentate.[65] Applying this methodology, we concluded that one nitrate is bound in an anisobidentate fashion in **1**·Zn-*trans* (Δd = 0.37 Å), while the other nitrate is undoubtedly a monodentate ligand (0.66 Å). Therefore, each zinc center in **1**·Zn-*trans* is six-coordinate, and the coordination structure at the metal is best described as a distorted octahedral geometry. The major structural distortion arises from the small biting angle [O1−Zn1−O2 55.1(3)°] of the bidentate nitrate ion. The bond lengths around the Zn^{II} centers were in the common range of similar complexes.[66,67] However, the Zn−N bond distances ranged between 2.058(8) and 2.228(7) Å, while the Zn−O lengths varied in a wide range from 2.091(7) to 2.468(7) Å.

The azobenzene linker of **1**·Zn-*trans* was eventually planar with respect to the PhN═NPh unit, as expected from the π conjugation, and the maximum deviation from the mean plane observed for the azo group was 0.086 Å. The N−N distance of the azobenzene linker was 1.240(10) Å, which was similar to that reported for an azobenzene complex.[68] The distance between the benzylic carbon atoms of the ligand was 12.08 Å, and that between the two Zn^{II} centers in the molecule was 17.87 Å. Each dinuclear unit was interlinked with the neighboring complexes through $\pi-\pi$ stacking between the pyridine rings, constructing a two-dimensional supramolecular sheet along the *ac* plane (Figure S2 in the Supporting Information).

Zn^{II} ions in mononuclear complexes with similar ligands have been reported to be five-coordinate, with varying geometry at the metal center from trigonal-bipyramidal to square-pyramidal geometry, depending on the position of the solvent and/or the counterion.[66,67] In **1**·Zn-*trans*, each zinc ion was situated in an octahedral environment, which was regulated by the bidentate coordination mode of one of the nitrate ions. Therefore, we can expect at least two water molecules to coordinate to each zinc center of **1**·Zn-*trans* in an aqueous solution.

Photoisomerization of Ligand 1 and Complex 1·Zn. The trans form of ligand **1** (**1**-*trans*) exhibited $\pi-\pi^*$ (337 nm) and $n-\pi^*$ (429 nm) absorption bands because of the azobenzene chromophore (Figure S3 in the Supporting Information). Irradiation of **1**-*trans* with UV light (320 nm < λ < 400 nm) led to the formation of its cis congener (**1**-*cis*), with a decrease in the intensity of the $\pi-\pi^*$ band and a concomitant increase in that of the $n-\pi^*$ band with isosbestic points at 278 and 420 nm.[46,49,50,53−55,57] Simultaneously, the absorption maximum of the $\pi-\pi^*$ band shifted slightly to a shorter wavelength in the cis form. The trans-to-cis photoisomerization of ligand **1** reached a photostationary state (PSS) after about 30 min of irradiation with UV light. Several ^{1}H NMR signals of the PSS state obtained after UV irradiation had shifted upfield compared to those of **1**-*trans*, as reported previously.[51] The ratio of the trans and cis forms of the ligand was calculated from the relative intensities of the shifted signals against the unaffected ones by photoisomerization. The trans/cis ratio of ligand **1** at the PSS obtained by UV irradiation of **1**-*trans* was estimated to be 20:80 (Figure S4 in the Supporting Information), where the cis form was the major isomer (abbreviated to **1**-*cis*-pss). Subsequent irradiation of **1**-*cis*-pss with visible light (λ > 420 nm) resulted in a PSS with the trans form as the predominant isomer (~80%; **1**-*trans*-pss), according to a similar NMR spectral analysis (Figure S4 in the Supporting Information). The trans/cis ratio at **1**-*trans*-pss was also estimated from the absorption spectra and the trans/cis ratio of **1**-*cis*-pss obtained from the ^{1}H NMR spectra. The absorption spectrum of

dx.doi.org/10.1021/ic201244y | Inorg. Chem. 2011, 50, 11437–11445

100% **1**-*cis* was calculated from the absorption spectra of **1**-*trans* and **1**-*cis*-pss and the trans/cis ratio at **1**-*cis*-pss obtained from the ^{1}H NMR spectra (Figure S3 in the Supporting Information). Next, the absorption spectrum of **1**-*trans*-pss was reproduced with the absorption spectrum of **1**-*trans* and the estimated spectrum of **1**-*cis*, resulting in a trans/cis ratio of 20:80, which matched very well that obtained from the ^{1}H NMR spectral analysis described above.

UV−vis spectroscopy was used to evaluate photoisomerization of complex **1**·Zn (Figure 2) because its ^{1}H NMR signals

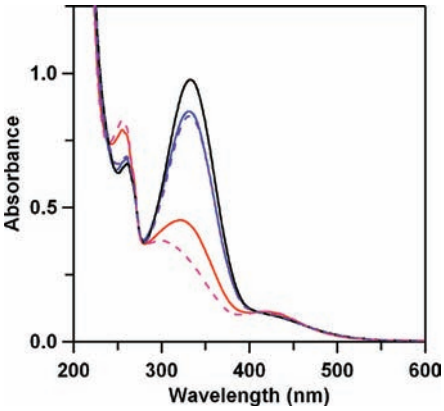

Figure 2. Absorption spectra of complex **1**·Zn (4.0×10^{-5} M). **1**·Zn-*trans* (black) is converted to a PSS by irradiation with UV light (**1**·Zn-*cis*-pss, red), and the obtained **1**·Zn-*cis*-pss is converted to another PSS by subsequent irradiation with visible light (**1**·Zn-*trans*-pss, blue). The estimated spectrum of 100% **1**·Zn-*cis* (broken pink) is calculated from the **1**·Zn-*trans* and **1**·Zn-*cis*-pss spectra and the cis/trans ratio of **1**·Zn-*cis*-pss obtained from the NMR data. The calculated spectrum of a mixture of 80% **1**·Zn-*trans* and 20% **1**·Zn-*cis* (broken purple) is also depicted.

were highly overlapped (Figure S1 in the Supporting Information). The trans/cis ratios of complex **1**·Zn at the PSSs obtained by UV (**1**·Zn-*cis*-pss) and visible light irradiation (**1**·Zn-*trans*-pss) were estimated to be trans/cis = 20:80 and 80:20, respectively. The trans-to-cis photoconversion of **1**·Zn-*trans* and cis-to-trans conversion of **1**·Zn-*cis* proceeded to the same extent as their corresponding forms of ligand **1** by UV and visible light irradiation, respectively. Photoisomerization of ligand **1** and complex **1**·Zn could be performed repeatedly, as reported for other compounds with azobenzene groups.[46,49,50,53−55,57] These results show that the azobenzene chromophore of the ligand undergoes effective photoisomerization, and therefore the spatial orientation of the coordinated Zn^{II} centers can be externally controlled by light. However, **1**·Zn-*cis* converts to the thermodynamically stable **1**·Zn-*trans* over time. A rate constant of 6.7×10^{-6} s^{-1} was obtained for the cis-to-trans conversion of complex **1**·Zn in an aqueous solution at 37 °C, where about 30% of the cis form converted to the trans form after incubation for 24 h (Figure S5 in the Supporting Information). No significant difference in the rate of cis-to-trans thermal conversion was observed between the absence and presence of DNA (Figure S6 in the Supporting Information), suggesting that electrostatic interactions between **1**·Zn-*cis* and DNA are not strong enough to affect thermal isomerization of the azo group (vide infra).

Complex 1·Zn Binding to DNA. Because binding of a metallocomplex to DNA is considered to be an important step in DNA cleavage, the binding abilities of **1**·Zn-*trans* and **1**·Zn-*cis*-pss to CT-DNA were measured by intensity changes in their $\pi-\pi^*$ absorption bands of the azobenzene chromophore at 337 and 323 nm, respectively (Figure 3). By the addition of CT-DNA

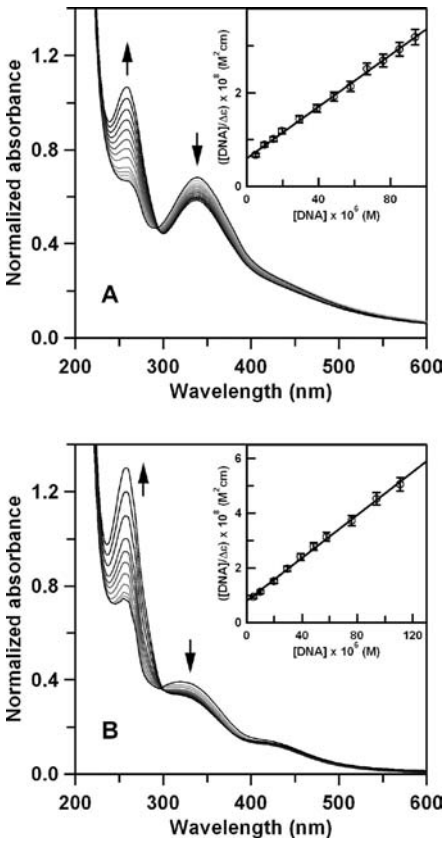

Figure 3. Absorption spectral changes upon the incremental addition of CT-DNA (1.5×10^{-3} M, 3.3−13.3 μL per scan) to complex **1**·Zn (2.5×10^{-5} M, 1.0 mL) in a 20 mM phosphate buffer (pH 7.5) at room temperature: (A) **1**·Zn-*trans* and (B) **1**·Zn-*cis*-pss. Inset: Plot of $[DNA]/\Delta\varepsilon$ versus [DNA] obtained by the absorption titration of CT-DNA with (A) **1**·Zn-*trans* and (B) **1**·Zn-*cis*-pss, respectively. Each absorption spectrum was normalized with the concentration of complex **1**·Zn at 2.5×10^{-5} M.

to either form of the complex in a 20 mM phosphate buffer (pH 7.5), only a moderate hypochromism was observed. The intrinsic binding constant (K_b) was determined with the following equation:[69]

$$[DNA]/(\varepsilon_a - \varepsilon_f) = [DNA]/(\varepsilon_b - \varepsilon_f) + 1/K_b(\varepsilon_b - \varepsilon_f)$$

where [DNA] is the concentration of the base pairs, ε_a is the observed extinction coefficient for the $\pi-\pi^*$ absorption band of the azobenzene moiety at each DNA concentration, ε_f is the extinction coefficient of the free complex, and ε_b is the extinction coefficient of the complex when fully bound to DNA. The K_b values for **1**·Zn-*trans* and **1**·Zn-*cis*-pss were obtained as $(4.6 \pm 0.1) \times 10^4$ and $(4.9 \pm 0.1) \times 10^4$ M^{-1}, respectively. The K_b values were similar between the trans and cis forms but were significantly lower than those reported for typical intercalators, indicating that complex **1**·Zn does not bind to DNA through an intercalation mode for either the trans or cis form.[70] However, in Figure 3, the increase in the absorbance with the addition of DNA was lower than expected, especially at the initial stages of DNA addition. For example, the difference between the absorbances at 260 nm of the

dx.doi.org/10.1021/ic201244y | Inorg. Chem. 2011, 50, 11437−11445

initial and final spectra in Figure 3B was 0.57, whereas it was estimated as 0.73 from the DNA concentration difference of 111 μM and ε = 6600 M^{-1} cm^{-1}. Because complexes **1**·Zn-*trans* and **1**·Zn-*cis*-pss show absorption at 260 nm (Figure 2), the decrease in the absorbance, mainly at the initial stage of DNA addition, may be due to the decrease in the absorption of the complex at 260 nm by the interaction with DNA.

To investigate the DNA binding affinity of **1**·Zn-*cis*-pss in more detail, its binding affinity with DNA was compared with that of EB by fluorescence spectroscopy. The emission intensity of EB decreases at the outside of the DNA strand because of the quenching effect by the solvent molecules, whereas it increases significantly by intercalating to DNA. Interaction of a complex with EB-bound DNA may decrease the emission intensity of EB by releasing EB from DNA, and therefore the reduction of the emission intensity can be used as a measure of the DNA binding propensity.[71] However, the fluorescence intensity did not decrease effectively by the addition of 2 equiv of **1**·Zn-*cis*-pss to EB-bound DNA, indicating that the complex does not bind to DNA through an intercalation mode (Figure S7 in the Supporting Information). These results support the hypothesis that compound **1**·Zn does not bind through an intercalation mode because the obtained binding constants of complex **1**·Zn to DNA were much smaller than that of EB. Electrostatic interaction is another major feature for small metal complexes to interact with DNA. The positive charges in complex **1**·Zn could lead the complex to interact with the anionic phosphodiester backbone of DNA. In fact, the binding constant of **1**·Zn-*cis*-pss to CT-DNA decreased from (4.9 ± 0.1) × 10^4 to (2.4 ± 0.2) × 10^4 M^{-1} by the addition of 200 mM NaCl (Figure S8 in the Supporting Information).

The binding constants of **1**·Zn to DNA were smaller than that reported for a nonintercalative dinuclear ruthenium complex with a charge of 4+ in total.[72] In aqueous solutions, water molecules and/or OH^- ions may replace the nitrate ligands in **1**·Zn, and two water/OH^- molecules would be coordinated to each Zn ion in **1**·Zn. The pK_a of the coordinated water/OH^- is about 7.9–8.35 in zinc complexes with one coordinated water molecule,[73] whereas the pK_a value of a zinc ion with two coordinated water molecules may show relatively dispersed values (for example, pK_a = 7.8 and 9.3).[74] An OH^- ion instead of a water molecule may coordinate to the zinc ion in **1**·Zn under the experimental conditions (pH 7.5). Therefore, **1**·Zn may be less charged than 4+ because of deprotonation of the coordinating water, and the binding constant to DNA may be smaller than that of the nonintercalative 4+ complex.

DNA Cleavage by Complex 1·Zn. The DNA cleavage properties of **1**·Zn-*trans* and **1**·Zn-*cis*-pss were studied using agarose gel electrophoresis with supercoiled pUC19 plasmid DNA. Although only a slight amount of nicked-circular DNA (form II) was produced even after incubation of supercoiled DNA (form I) with 100 μM **1**·Zn-*trans* at 37 °C for 24 h, **1**·Zn-*cis*-pss showed efficient DNA cleavage activity under the same conditions (Figure 4). These results demonstrate that the cis complex has a higher DNA cleavage activity than its trans congener. In the cis form, two metal centers are sufficiently close to each other, and therefore they can play a cooperative role in DNA cleavage. We attribute the higher DNA cleavage activity of the cis complex to the cooperation of two closely associated Zn^{II} centers, while the metal centers are positioned relatively far way from each other in the trans form (17.87 Å). Although **1**·Zn-*cis* converts to **1**·Zn-*trans* thermodynamically (rate constant, 6.7 × 10^{-6} s^{-1}), about 50% of the supercoiled

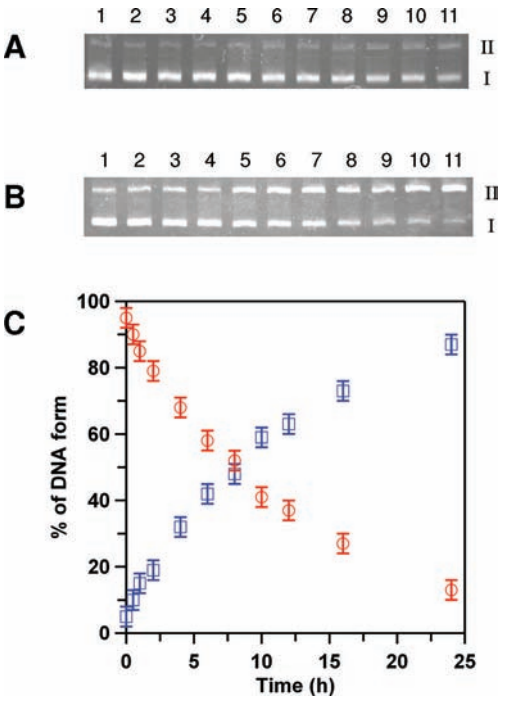

Figure 4. Time courses of cleavage of pUC19 DNA by complex **1**·Zn (100 μM) in a 20 mM phosphate buffer (pH 7.5) at 37 °C. Agarose gel electrophoresis patterns of pUC19 DNA (1 μg) are shown at various reaction times for (A) **1**·Zn-*trans* and (B) **1**·Zn-*cis*-pss, respectively: Lanes 1–11: reaction times of 0, 1, 2, 3, 4, 6, 8, 10, 12, 16, and 24 h, respectively. (C) Plots of percentages of supercoiled (red) and nicked-circular (blue) DNA versus reaction time. I and II represent DNA forms 1 and 2, respectively.

DNA converted to the nicked-circular DNA after 8 h of incubation with 100 μM **1**·Zn-*cis*-pss (Figure 4C). However, no linear DNA was produced even after incubation of **1**·Zn-*cis*-pss with DNA for 24 h.

The DNA cleavage activity was remarkably different between the cis and trans forms of complex **1**·Zn, although both forms had similar binding affinities toward DNA. Our previous molecular modeling study showed that the intramolecular separation between the benzylic carbon atoms of the azobenzene chromophore in the cis form is ~8 Å, whereas they are ~12 Å away from each other in the trans form.[51] The Cu^{II}-bound dipeptides in an azobenzene-linked complex were far away from each other in the trans form and were not favorable for cooperation and DNA cleavage, while they were oriented toward each other in the cis form and exhibited effective cooperation to cleave DNA. In fact, the X-ray crystal structure of **1**·Zn-*trans* showed that the intramolecular distance between the benzylic carbon atoms of its azobenzene group was 12.08 Å. One can expect a cooperation effect in the cis configuration of complex **1**·Zn similar to that in the Cu^{II}-bound dipeptides linked with an azobenzene group. The higher reactivity of the cis form of complex **1**·Zn shows the importance of the cooperation of the two Zn^{II} centers for DNA cleavage.

DNA Interaction of Complex 1·Zn in the Cis Form. The concentration dependence of **1**-*cis*-pss from 10 to 150 μM on the DNA cleavage activity exhibited a saturation curve (Figure S9 in the Supporting Information). These results suggested that the DNA cleavage reaction proceeds through a DNA–complex adduct, where interaction of the metal center with DNA is important for DNA cleavage. In order to obtain

dx.doi.org/10.1021/ic201244y | *Inorg. Chem.* 2011, 50, 11437–11445

information on the interaction between **1**·Zn-*cis* and DNA, DNA cleavage experiments were carried out in the presence of a major groove binding agent, methyl green, and a minor groove binder, DAPI. DNA cleavage was not affected by methyl green but was affected by DAPI, suggesting that **1**·Zn-*cis* binds at the minor grooves of DNA (Figure 5).

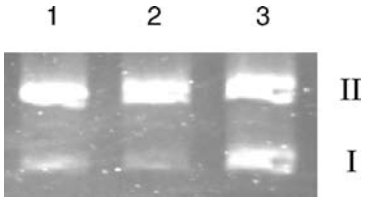

Figure 5. Agarose gel electrophoresis patterns of pUC19 DNA (1 μg) after 24 h of incubation with **1**·Zn-*cis*-pss (100 μM) in a 20 mM phosphate buffer (pH 7.5) at 37 °C. Lane 1: in the absence of methyl green and DAPI. Lane 2: in the presence of methyl green (50 μM). Lane 3: in the presence of DAPI (50 μM). I and II represent DNA forms 1 and 2, respectively.

The binding constant of **1**·Zn-*cis*-pss to CT-DNA decreased with the addition of NaCl (Figure S8 in the Supporting Information), indicating the importance of electrostatic interaction between the positively charged Zn^{II} centers and the anionic phosphate backbone of DNA. The DNA cleavage efficiency was also decreased by the addition of NaCl (Figure S10A in the Supporting Information). A similar phenomenon has been observed in other positively charged metallocompounds,[26,38] and electrostatic interaction may play a significant role in the binding of **1**·Zn-*cis* at the minor groove region of DNA, which is important for the DNA cleavage activity.[75]

Hydrolytic DNA Cleavage by Complex 1·Zn in the Cis Form. The use of the Zn^{II} ion allows us to discard the possibility of metal-ion-driven oxidative cleavage, and therefore the complex may cleave DNA hydrolytically. The pH dependence of the DNA cleavage activity by **1**·Zn-*cis*-pss exhibited a bell-shaped curve, possessing a maximum at pH 8.5. The pH value of the maximum activity was close to the pK_a values of reported zinc complexes having similar coordination environments (pK_a, about 7.9−8.35 for a single-coordinated water molecule;[73] Figure S11 in the Supporting Information).[66,72] This pH-dependence profile is typical for artificial nucleases, which promote hydrolytic DNA cleavage.[33,37,76] These results suggest that metal hydroxide coordination of the complex is involved in the course of hydrolytic cleavage. Such species may be formed by deprotonation of at least one water molecule, which is coordinated to the metal center.[77] However, the hydroxide bound to the metal, consequently, reduces the charge on the metal complex, which is presumably unfavorable for the binding of the complex to the negatively charged nucleic acid.[78] Therefore, the decrease in the hydrolytic activity at higher pH values is possibly due to the decrease in the charge of the complex. It is noteworthy that the cleavage activity decreased significantly in the presence of nitrate ions (Figure S10B in the Supporting Information). The X-ray crystal structure revealed that the nitrate ions bind firmly to the zinc ions in complex **1**·Zn (Figure 1). Therefore, nitrate ions may coordinate to the zinc centers in an aqueous solution at high $NaNO_3$ concentrations and block the coordination sites for water molecules, resulting in a significance decrease in the DNA cleavage activity. These results also show the importance of water/hydroxide ion coordination to the zinc centers for DNA cleavage.

The present results indicate that the nonenzymatic hydrolysis of a phosphodiester bond of DNA can be performed effectively by orienting two zinc ions appropriately. In fact, the DNA cleavage activity of the cis form of complex **1**·Zn was higher than that of its trans congener, and its cleavage activity was affected by the pH and the addition of NaCl. To explain the cooperative role of the two zinc centers in the cis form on DNA cleavage, a possible mechanism is proposed (Scheme 3): The

Scheme 3. Proposed Scheme for DNA Hydrolytic Cleavage by the Cis Form of Complex 1·Zn

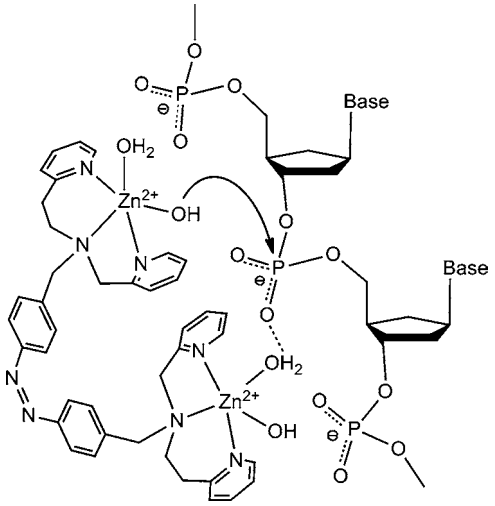

two Zn^{II} centers are positioned close to each other in the cis complex, and the positively charged zinc centers guide the complex to interact with the negatively charged phosphate groups of the DNA backbone by electrostatic interaction. In this conformation, the two zinc centers both interact with the same phosphate group in the DNA backbone. While the water molecule(s) at one zinc center interact with the oxygen atom of the phosphate group, a hydroxide ion bound at the other zinc center operates a nucleophilic attack to the phosphorus atom of the phosphate group, initiating DNA cleavage.[79,80]

CONCLUSIONS

We synthesized a novel photoactive dinuclear zinc(II) complex with an azobenzene linker. The X-ray crystal structure of its trans form showed that each zinc center exhibits a distorted octahedral geometry, in which two metal centers were situated far away from each other (17.87 Å). The spatial disposition of the two metal centers was externally controlled by photoisomerization of the azobenzene chromophore. The binding affinities of both the cis and trans forms of the complex to DNA were similar, where the positively charged complex presumably interacted electrostatically with the negatively charged phosphate groups of DNA. However, the complex in the cis form exhibited hydrolytic DNA cleavage activity, whereas the activity in the trans form was negligible. The efficient DNA cleavage activity of the cis form is attributed to the cooperation of two zinc centers closely located between each other. The DNA cleavage activity of the cis complex was decreased by the addition of a minor groove binder, DAPI, showing that the complex binds to the minor groove of DNA. These results show the importance of the cooperation of zinc ions, which can be photoregulated by a photoisomerizable linker such as an azobenzene chromophore.

dx.doi.org/10.1021/ic201244y | *Inorg. Chem.* 2011, 50, 11437–11445

■ ASSOCIATED CONTENT

Supporting Information

X-ray crystallographic data in CIF format and additional results of photoisomerization, DNA binding, and cleavage experiments. This material is available free of charge via the Internet at http://pubs.acs.org.

■ AUTHOR INFORMATION

Corresponding Author

*E-mail: hirota@ms.naist.jp. Fax: +81-743-72-6110.

■ ACKNOWLEDGMENTS

We thank Syouhei Katao and Yuriko Nishiyama, Nara Institute of Science and Technology, for carrying out X-ray diffraction and ESI-MS measurements. We are also grateful to Leigh McDowell, Nara Institute of Science and Technology, for his advice on the manuscript preparation. This work was partially supported by Grants-in-Aid for Scientific Research from MEXT (Priority Areas, No. 23107723), JSPS (Category B No.21350095), JST, Sankyo Foundation of Life Science, and Toray Science Foundation (all to S.H.). A.P. is thankful to JSPS for a fellowship.

■ REFERENCES

(1) Dandliker, P. J.; Holmlin, R. E.; Barton, J. K. *Science* **1997**, *275*, 1465−1468.
(2) Krämer, R. *Coord. Chem. Rev.* **1999**, *182*, 243−261.
(3) Cowan, J. A. *Curr. Opin. Chem. Biol.* **2001**, *5*, 634−642.
(4) Mancin, F.; Scrimin, P.; Tecilla, P.; Tonellato, U. *Chem. Commun.* **2005**, 2540−2548.
(5) Jiang, Q.; Xiao, N.; Shi, P.; Zhu, Y.; Guo, Z. *Coord. Chem. Rev.* **2007**, *251*, 1951−1972.
(6) Mancin, F.; Tecilla, P. In *Metal Complex−DNA Interactions*; Hadjiliadis, N., Sletten, E., Eds.; John Wiley & Sons, Ltd.: Chichester, U.K., 2009; pp 369−394.
(7) Sasmal, P. K.; Saha, S.; Majumdar, R.; Dighe, R. R.; Chakravarty, A. R. *Inorg. Chem.* **2010**, *49*, 849−859.
(8) Pogozelski, W. K.; Tullius, T. D. *Chem. Rev.* **1998**, *98*, 1089−1108.
(9) Burrows, C. J.; Muller, J. G. *Chem. Rev.* **1998**, *98*, 1109−1152.
(10) Li, L.; Karlin, K. D.; Rokita, S. E. *J. Am. Chem. Soc.* **2005**, *127*, 520−521.
(11) Bales, B. C.; Pitie, M.; Meunier, B.; Greenberg, M. M. *J. Am. Chem. Soc.* **2002**, *124*, 9062−9063.
(12) Jin, Y.; Cowan, J. A. *J. Am. Chem. Soc.* **2005**, *127*, 8408−8415.
(13) Maheswari, P. U.; Roy, S.; den Dulk, H.; Barends, S.; van Wezel, G.; Kozlevcar, B.; Gamez, P.; Reedijk, J. *J. Am. Chem. Soc.* **2006**, *128*, 710−711.
(14) García-Giménez, J. L.; Alzuet, G.; Gonzalez-Álvarez, M.; Castiñeiras, A.; Liu-González, M.; Borrás, J. *Inorg. Chem.* **2007**, *46*, 7178−7188.
(15) Rajendiran, V.; Karthik, R.; Palaniandavar, M.; Stoeckli-Evans, H.; Periasamy, V. S.; Akbarsha, M. A.; Srinag, B. S.; Krishnamurthy, H. *Inorg. Chem.* **2007**, *46*, 8208−8221.
(16) Jin, Y.; Lewis, M. A.; Gokhale, N. H.; Long, E. C.; Cowan, J. A. *J. Am. Chem. Soc.* **2007**, *129*, 8353−8361.
(17) Lu, Z.-L.; Liu, C. T.; Neverov, A. A.; Brown, R. S. *J. Am. Chem. Soc.* **2007**, *129*, 11642−11652.
(18) Fitzsimons, M. P.; Barton, J. K. *J. Am. Chem. Soc.* **1997**, *119*, 3379−3380.
(19) Wilson, B.; Gude, L.; Fernandez, M. J.; Lorente, A.; Grant, K. B. *Inorg. Chem.* **2005**, *44*, 6159−6173.
(20) Maheswari, P. U.; Barends, S.; Ozalp-Yaman, S.; de Hoog, P.; Casellas, H.; Teat, S. J.; Massera, C.; Lutz, M.; Spek, A. L.; van Wezel, G. P.; Gamez, P.; Reedijk, J. *Chem.—Eur. J.* **2007**, *13*, 5213−5222.
(21) Bonomi, R.; Selvestrel, F.; Lombardo, V.; Sissi, C.; Polizzi, S.; Mancin, F.; Tonellato, U.; Scrimin, P. *J. Am. Chem. Soc.* **2008**, *130*, 15744−15745.
(22) Komiyama, M.; Takeda, N.; Shigekawa, H. *Chem. Commun.* **1999**, 1443−1451.
(23) Copeland, K. D.; Fitzsimons, M. P.; Houser, R. P.; Barton, J. K. *Biochemistry* **2002**, *41*, 343−356.
(24) He, J.; Sun, J.; Mao, Z.-W.; Ji, L.-N.; Sun, H. *J. Inorg. Biochem.* **2009**, *103*, 851−858.
(25) Boseggia, E.; Gatos, M.; Lucatello, L.; Mancin, F.; Moro, S.; Palumbo, M.; Sissi, C.; Tecilla, P.; Tonellato, U.; Zagotto, G. *J. Am. Chem. Soc.* **2004**, *126*, 4543−4549.
(26) Nomura, A.; Sugiura, Y. *J. Am. Chem. Soc.* **2004**, *126*, 15374−15375.
(27) Katada, H.; Komiyama, M. *ChemBioChem* **2009**, *10*, 1279−1288.
(28) Liu, C.; Wang, M.; Zhang, T.; Sun, H. *Coord. Chem. Rev.* **2004**, *248*, 147−168.
(29) Xiang, Q.-X.; Zhang, J.; Liu, P.-Y.; Xia, C.-Q.; Zhou, Z.-Y.; Xie, R.-G.; Yu, X.-Q. *J. Inorg. Biochem.* **2005**, *99*, 1661−1669.
(30) Xia, C.-Q.; Jiang, N.; Zhang, J.; Chen, S.-Y.; Lin, H.-H.; Tan, X.-Y.; Yue, Y.; Yu, X.-Q. *Bioorg. Med. Chem.* **2006**, *14*, 5756−5764.
(31) Mancin, F.; Tecilla, P. *New J. Chem.* **2007**, *31*, 800−817.
(32) Rey, N. A.; Neves, A.; Bortoluzzi, A. J.; Pich, C. T.; Terenzi, H. *Inorg. Chem.* **2007**, *46*, 348−350.
(33) Sheng, X.; Lu, X.-M.; Chen, Y.-T.; Lu, G.-Y.; Zhang, J.-J.; Shao, Y.; Liu, F.; Xu, Q. *Chem.—Eur. J.* **2007**, *13*, 9703−9712.
(34) Bazzicalupi, C.; Bencini, A.; Bonaccini, C.; Giorgi, C.; Gratteri, P.; Moro, S.; Palumbo, M.; Simionato, A.; Sgrignani, J.; Sissi, C.; Valtancoli, B. *Inorg. Chem.* **2008**, *47*, 5473−5484.
(35) Liu, C.; Wang, L. *Dalton Trans.* **2009**, 227−239.
(36) Camargo, M. A.; Neves, A.; Bortoluzzi, A. J.; Szpoganicz, B.; Fischer, F. L.; Terenzi, H.; Serra, O. A.; Santos, V. G.; Vaz, B. G.; Eberlin, M. N. *Inorg. Chem.* **2010**, *49*, 6013−6025.
(37) Sissi, C.; Rossi, P.; Felluga, F.; Formaggio, F.; Palumbo, M.; Tecilla, P.; Toniolo, C.; Scrimin, P. *J. Am. Chem. Soc.* **2001**, *123*, 3169−3170.
(38) Sheng, X.; Guo, X.; Lu, X.-M.; Lu, G.-Y.; Shao, Y.; Liu, F.; Xu, Q. *Bioconjug. Chem.* **2008**, *19*, 490−498.
(39) Hough, E.; Hansen, L. K.; Birknes, B.; Jynge, K.; Hansen, S.; Hordvik, A.; Little, C.; Dodson, E.; Derewenda, Z. *Nature* **1989**, *338*, 357−360.
(40) Lahm, A.; Volbeda, A.; Suck, D. *J. Mol. Biol.* **1990**, *215*, 207−210.
(41) Davies, J. F. 2nd; Hostomska, Z.; Hostomsky, Z.; Jordan, S. R.; Matthews, D. A. *Science* **1991**, *252*, 88−95.
(42) Kim, E. E.; Wyckoff, H. W. *J. Mol. Biol.* **1991**, *218*, 449−464.
(43) Wilcox, D. E. *Chem. Rev.* **1996**, *96*, 2435−2458.
(44) Desai, N. A.; Shankar, V. *FEMS Microbiol. Rev.* **2003**, *26*, 457−491.
(45) Weston, J. *Chem. Rev.* **2005**, *105*, 2151−2174.
(46) Woolley, G. A. *Acc. Chem. Res.* **2005**, *38*, 486−493.
(47) Hamill, A. C.; Wang, S. C.; Lee, C. T. Jr. *Biochemistry* **2005**, *44*, 15139−15149.
(48) Kusebauch, U.; Cadamuro, S. A.; Musiol, H. J.; Lenz, M. O.; Wachtveitl, J.; Moroder, L.; Renner, C. *Angew. Chem., Int. Ed.* **2006**, *45*, 7015−7018.
(49) Asanuma, H.; Liang, X.; Nishioka, H.; Matsunaga, D.; Liu, M.; Komiyama, M. *Nat. Protoc.* **2007**, *2*, 203−212.
(50) Dohno, C.; Uno, S. N.; Nakatani, K. *J. Am. Chem. Soc.* **2007**, *129*, 11898−11899.
(51) Prakash, H.; Shodai, A.; Yasui, H.; Sakurai, H.; Hirota, S. *Inorg. Chem.* **2008**, *47*, 5045−5047.
(52) Takahashi, I.; Honda, Y.; Hirota, S. *Angew. Chem., Int. Ed.* **2009**, *48*, 6065−6068.
(53) Hoppmann, C.; Seedorff, S.; Richter, A.; Fabian, H.; Schmieder, P.; Ruck-Braun, K.; Beyermann, M. *Angew. Chem., Int. Ed.* **2009**, *48*, 6636−6639.

(54) Zhang, F.; Zarrine-Afsar, A.; Al-Abdul-Wahid, M. S.; Prosser, R. S.; Davidson, A. R.; Woolley, G. A. *J. Am. Chem. Soc.* **2009**, *131*, 2283−2289.
(55) Kreger, K.; Wolfer, P.; Audorff, H.; Kador, L.; Stingelin-Stutzmann, N.; Smith, P.; Schmidt, H. W. *J. Am. Chem. Soc.* **2010**, *132*, 509−516.
(56) Schierling, B.; Noel, A. J.; Wende, W.; Hien le, T.; Volkov, E.; Kubareva, E.; Oretskaya, T.; Kokkinidis, M.; Rompp, A.; Spengler, B.; Pingoud, A. *Proc. Natl. Acad. Sci. U.S.A.* **2010**, *107*, 1361−1366.
(57) Beharry, A. A.; Woolley, G. A. *Chem. Soc. Rev.* **2011**, *40*, 4422−4437.
(58) Ren, Y.-w.; Wu, A.-z.; Liu, H.-y.; Jiang, H.-f. *Transition Met. Chem.* **2010**, *35*, 191−195.
(59) Sheldrick, G. M. *Acta Crystallogr., Sect. A* **2008**, *64*, 112−122.
(60) Reichmann, M. E.; Rice, S. A.; Thomas, C. A.; Doty, P. *J. Am. Chem. Soc.* **1954**, *76*, 3047−3053.
(61) Rammo, J.; Hettich, R.; Roigk, A.; Schneider, H.-J. *Chem. Commun.* **1996**, 105−107.
(62) González-Álvarez, M.; Alzuet, G.; Borrás, J.; Macías, B.; Castiñeiras, A. *Inorg. Chem.* **2003**, *42*, 2992−2998.
(63) Wittung, P.; Nielsen, P.; Nordén, B. *J. Am. Chem. Soc.* **1996**, *118*, 7049−7054.
(64) Trotta, E.; Del Grosso, N.; Erba, M.; Paci, M. *Biochemistry* **2000**, *39*, 6799−6808.
(65) Parkin, G. *Chem. Rev.* **2004**, *104*, 699−767.
(66) Gultneh, Y.; Khan, A. R.; Blaise, D.; Chaudhry, S.; Ahvazi, B.; Marvey, B. B.; Butcher, R. J. *J. Inorg. Biochem.* **1999**, 7−18.
(67) Balamurugan, V.; Hundal, M. S.; Mukherjee, R. *Chem.—Eur. J.* **2004**, *10*, 1683−1690.
(68) Bardají, M.; Barrio, M.; Espinet, P. *Dalton Trans.* **2011**, *40*, 2570−2577.
(69) Wolfe, A.; Shimer, G. H. Jr.; Meehan, T. *Biochemistry* **1987**, *26*, 6392−6396.
(70) Lepecq, J. B.; Paoletti, C. *J. Mol. Biol.* **1967**, *27*, 87−106.
(71) Barton, C. V. K. J. K.; Turro, N. J. *J. Am. Chem. Soc.* **1985**, *107*, 5518−5523.
(72) Lutterman, D. A.; Chouai, A.; Liu, Y.; Sun, Y.; Stewart, C. D.; Dunbar, K. R.; Turro, C. *J. Am. Chem. Soc.* **2008**, *130*, 1163−1170.
(73) Subat, M.; Woinaroschy, K.; Gerstl, C.; Sarkar, B.; Kaim, W.; Konig, B. *Inorg. Chem.* **2008**, *47*, 4661−4668.
(74) Nazarenko, V.; Antonovich, V. *Zh. Neorg. Khim.* **1978**, *23*, 1787−1791.
(75) Humphreys, K. J.; Karlin, K. D.; Rokita, S. E. *J. Am. Chem. Soc.* **2002**, *124*, 8055−8066.
(76) Tjioe, L.; Joshi, T.; Brugger, J.; Graham, B.; Spiccia, L. *Inorg. Chem.* **2011**, *50*, 621−635.
(77) Kimura, E. *Curr. Opin. Chem. Biol.* **2000**, *4*, 207−213.
(78) Misra, V. K.; Honig, B. *Proc. Natl. Acad. Sci. U.S.A.* **1995**, *92*, 4691−4695.
(79) Hegg, E. L.; Burstyn, J. N. *Coord. Chem. Rev.* **1998**, *173*, 133−165.
(80) Dupureur, C. M. *Curr. Opin. Chem. Biol.* **2008**, *12*, 250−255.